J. Mt. Sci. (2012) 9: 853–868
DOI: 10.1007/s11629-012-2419-1

Snow Cover Variation and Streamflow Simulation in a Snow-fed River Basin of the Northwest Himalaya

Vaibhav SHARMA[1], V.D. MISHRA[1], P.K. JOSHI[2]

1 Snow and Avalanche Study Establishment, Him Parisar, Sector 37A, Chandigarh 160036, India

2 TERI University, New Delhi-110070, India

** Corresponding author, e-mail: vaibhavsharma51@gmail.com*

Abstract: Snowmelt is an important component of any snow-fed river system. The Jhelum River is one such transnational mountain river flowing through India and Pakistan. The basin is minimally glacierized and its discharge is largely governed by seasonal snow cover and snowmelt. Therefore, accurate estimation of seasonal snow cover dynamics and snowmelt-induced runoff is important for sustainable water resource management in the region. The present study looks into spatio-temporal variations of snow cover for past decade and stream flow simulation in the Jhelum River basin. Snow cover extent (SCE) was estimated using MODIS (Moderate Resolution Imaging Spectrometer) sensor imageries. Normalized Difference Snow Index (NDSI) algorithm was used to generate multi-temporal time series snow cover maps. The results indicate large variation in snow cover distribution pattern and decreasing trend in different sub-basins of the Jhelum River. The relationship between SCE-temperature, SCE-discharge and discharge-precipitation was analyzed for different seasons and shows strong correlation. For streamflow simulation of the entire Jhelum basin Snow melt Runoff Model (SRM) used. A good correlation was observed between simulated stream flow and in-situ discharge. The monthly discharge contribution from different sub-basins to the total discharge of the Jhelum River was estimated using a modified version of runoff model based on temperature-index approach developed for small watersheds. Stream power — an indicator of the erosive capability of streams was also calculated for different sub-basins.

Received: 19 July 2012
Accepted: 18 October 2012

Keywords: Snow cover extent (SCE); Streamflow; Snow Melt Runoff Model (SRM); Normalized Difference Snow Index (NDSI); Jhelum basin; Moderate Resolution Imaging Spectrometer (MODIS)

Introduction

The Jhelum River is one of the main tributaries of the Indus and is a strategically important river of the north-west Himalaya. It is a principal source of irrigation in the plains of Punjab (Pakistan) having a substantial agricultural water deficit (Archer and Fowler 2008). The Jhelum originates at Verinag in Banihal sub-basin in the south-eastern part of the Kashmir valley. After rising from Banihal, it receives tributaries from the Greater Himalayan Range from east and Pirpanjal range from western side. The total length of the Jhelum River in India is 230 km. It flows northwards, from source to Wullar Lake and further down towards south-westwards. The river maintains a gentle gradient in the entire valley till it enters Wullar Lake which further attenuates its flow and drains towards Pakistan. Then Jhelum is joined by its other main tributaries Kunhar and the Kishanganga. The Jhelum significantly affects the regional economic and ecological systems. The discharge of the Jhelum River is primarily controlled by snowmelt in spring–summer season and by Indian south-west monsoon during monsoon season. During winter season Jhelum

basin receives heavy snowfall which results in delayed low river discharge.

Snow cover in a basin strongly indicates the amount of water likely to be yielded in the form of future runoff (Maurer et al. 2003; Tekeli et al. 2005). In addition, snow cover is also considered as an important component of surface radiation balance and climatological systems of a region (Foster et al. 1996; Yang et al. 1999; Salomonson and Appel 2004). The studies suggest that snow cover in the Himalaya could also affect the intensity of monsoon during July–September months (Immerzeel et al. 2009). Researchers (Blandford 1884; Kriplani et al. 2004; Shaman et al. 2005) have reported the tele-connection of the Himalayan snow cover with the Indian monsoonal rainfall. Furthermore, unexpected and sudden increase in snow cover may also lead to loss of man and material from snow avalanche, flash floods caused by rapid snow melt (Ramamoorthi and Haefner 1991) and crop damage due to change in soil thermal regimes (Zhang et al. 2010). Therefore, knowledge of dynamic snow cover changes and modeling of snowmelt is of major importance.

Accurate estimation of snow cover extent is a tedious task in mountainous terrain. Remote sensing is a promising tool for monitoring spatial and temporal changes at various scales. Variety of scientific studies has been carried out in the past using multi-spectral sensors like Landsat MSS (Multispectral Scanner System), TM (Thematic Mapper) and SPOT (Système Probatoire d'Observation de la Terre) data. These medium resolution sensors carry certain limitations like band saturation, small swath, unsuitable temporal and spectral resolution (Xiao et al. 2002 and 2004; Rutger et al. 2004; Kulkarni et al. 2006). NOAA AVHRR (National Oceanic and Atmospheric Administration Advance Very High Resolution Radiometer) data is widely accepted due to its high temporal resolution. However, this sensor still has low spatial resolution, limited scope for atmospheric correction effects and scattering due to aerosols and water vapors (Fitzharris and McAlevey 1999; Zhang et al. 2005 and 2010). Airborne LIDAR (Light Detection and Ranging) also represents an advance technology for snow cover mapping but again with expanse of scale limitations (Trujilo et al. 2007; Homan et al. 2011). MODIS is a sensor providing wide range of spectral resolution, medium spatial resolution and an alternate to above mentioned issues. Therefore, MODIS data was used in this study for estimation of SCE in Jhelum basin in last decade (2000–11). The estimated SCE values for the years between 2004 and 2009 were used for streamflow simulation of Jhelum basin.

Earlier similar snowmelt studies based on temperature-index approach have been conducted in various Himalayan River basin using different hydrological models. UBC (University of British Columbia) watershed model was used to estimate the snow and glacier melt during spring and summer season (Singh and Quick 1993). Suitability of snowmelt runoff simulation model HEC-1 (Hydrologic Engineering Center) and Clarke unit hydrograph option was tested on the Beas sub-basin (Verdhen and Prasad 1993). Jain et al. (1998) has used SLURP **(**Semi-distributed Land Use-based Runoff Processes) model to calculate the availability of water in the Satluj river basin. Rathore et al. (2009) calculated the effect of 1°C rise in temperature on the changes in the runoff and hydro-power potential of the Satluj river basin. However such estimates studies are not reported for the Jhelum river basin.

Snowmelt runoff model (SRM) (Martinec 1975) is a conceptual and deterministic degree day model. It has been successfully applied in the Himalayan river basins of various sizes and elevation. Kumar et al. (1991) applied SRM model in the Beas basin and found good correlation between observed and calculated stream flow. Prasad and Roy (2005) have simulated snowmelt runoff of the Beas River and have also calculated the basin runoff coefficients. Li and Williams (2008) have applied SRM with short-wave solar radiation and snow albedo in arid watershed of the Tarim basin. Immerzeel et al. (2009) successfully applied the SRM model in the upper Indus basin and has concluded that hydrology of the basin is being affected by regional warming due to accelerated glacial melting and snowmelt. Butt and Bilal (2011) has simulated the Astore river discharge using SRM model.

Unlike other northern rivers, Jhelum River has received less scientific research attention for monitoring of snow cover variation and streamflow simulation. Due to lack of climatic and geographical database, few hydrological studies

have been conducted at the regional level in the Jhelum basin of Jammu and Kashmir (India). Archer and Fowler (2004) have analyzed long term spatial variation in precipitation and have found relation between winter precipitation and summer runoff in the upper Indus basin. Archer and Fowler (2008) has also investigated the links between local climate and runoff in the upper Jhelum basin but has concentrated only on the seasonal forecasting of spring and summer inflows at Mangla Dam (Pakistan). Till present no snowmelt simulation study has been reported of the Jhelum River. Hence in the present study for the first time snowmelt simulation is attempted for the Jhelum basin and its corresponding sub-basins.

The tributaries of the Jhelum River carries heavy sediment load during flood season. The eroded sediments carried by stream flow are minimally deposited on the river bed and remaining quantity is transported for some distance in downstream areas and eventually deposited. This river action when remain continuous for long can change river flow and path. Stream power is a physically based measure of river sediment transport capacity and an indicator of river energy budget. It was estimated for different sub-basins of Jhelum River using average monthly simulated discharge. Thus, the understanding of geographical and seasonal variation of the stream power is important for informed decision making about the quantitative river system modeling.

The present study was carried out with multiple objectives, (a) snow cover variation in the Jhelum basin and in its four sub-basins was analyzed using remote sensing techniques (b) streamflow of the Jhelum River was estimated using SRM model developed by Martinec (1975), (c) streamflow was simulated for different ungauged sub-basins of the Jhelum River based on run-off model developed by Kulkarni et al. (2002), (d) estimation of streampower of different sub-basins of Jhelum River.

1 Basin information

The study area comprises of the Jhelum basin up to the Safapora discharge measurement site located in Jammu and Kashmir (India). The selected catchment of the Jhelum River lies between 33°22'30" N to 34°30'0" N latitude and 74°15'0" E to 75°31'34" E longitude. It spans a total area of 9,508 km² out of which 1.2% is glaciated, 13.1% is forest covered and 25% is covered by shrubs-grassy vegetation with dominant southern facing slopes.

Figure 1 shows the geographic setting of study area with the details of different sub-basins (Banihal, Gulmarg, Pahalgam, Sind) and various metrological and hydrological observatories. The Banihal and Gulmarg are situated on the lee-ward side of the Pirpanjal range whereas Pahalgam and Sind lie on the windward side of the Greater Himalayan range. The 48% of the basin area is a low-lying valley region. The elevation in the basin ranges from 1,500 m to 5,700 m. The physiographic characteristics of different sub-basins are shown in Table 1.

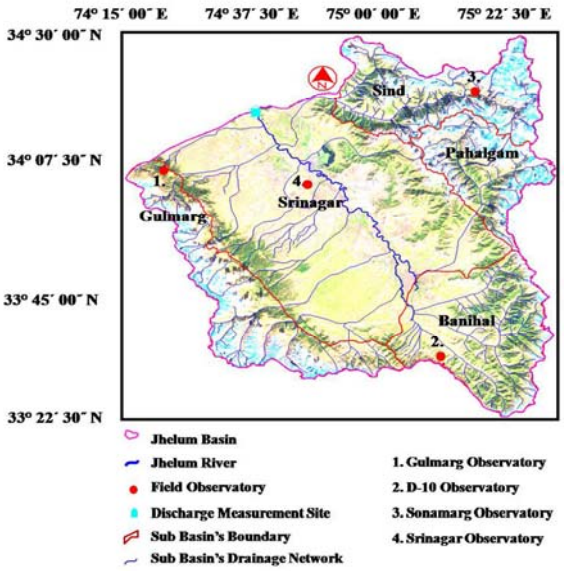

Figure 1 Study Area

1.1 Basin climatic regime

The meteorological data used in the present work was recorded at four SASE (Snow and Avalanche Study Establishment) field observatories in snow bound region. Each observatory is situated at mean altitude of a sub-basin of Jhelum basin. The overall climatology of the Jhelum basin is efficiently represented by all four observatories. The summary of these observatories are given in

Table 1 Physiographic characteristics of different sub-basins and valley region of Jhelum River basin

Physiographic characteristic	Sind	Pahalgam	Banihal	Gulmarg	Valley
Area (km²)	1,221	790	1,481	1,461	4,555
Mean elevation (m)	3,240	3,345	2,567	3,034	1,742
Forest cover (km²)	122.1	94.8	414.6	248.3	819.9
Glaciated area (km²)	65	35	0	18	0

Table 2 Salient features of hydrological and metrological observatories in Jhelum Basin

Items	Observatories				
	Safapora	D-10	Gulmarg	Sonamarg	Srinagar
Altitude (m)	1,600	2,823	2,986	3,185	1,649
Basin/Region	Entire basin	Banihal	Gulmarg	Pahalgam, Sind	Valley
Data Type	Streamflow	Metrological	Metrological	Metrological	Metrological
Organization	CWC	SASE	SASE	SASE	SASE

Table 2. In order to understand the basin climatology and seasonal cycles of the Jhelum basin, these parameters are further presented.

a) Temperature: Figure 2 shows the mean monthly temperature regime in Jhelum basin. The basin records very low temperature, with mean temperatures between temperatures -1 °C to -5 °C during December to February months. Relatively warmer temperature (2 °C - 10 °C) exists during March to June months. The highest temperature was recorded in July or August with temperature rising to 16 °C in September month followed by a gradual decrease.

b) Precipitation: Similar to temperature strong seasonal variability exists for precipitation over the Jhelum basin (Figure 2). The entire precipitation cycle can be classified as: October–February (winter period), March–June (spring–summer period) and July–September (monsoon period). Precipitation in winter period is caused by western disturbances. These are the extra-tropical weather system originating in mid-latitudinal region in Caspian Sea. In early winter high pressure area is created over the entire northern region due cold-dry climate. This instigates movement of north-westerly systems towards

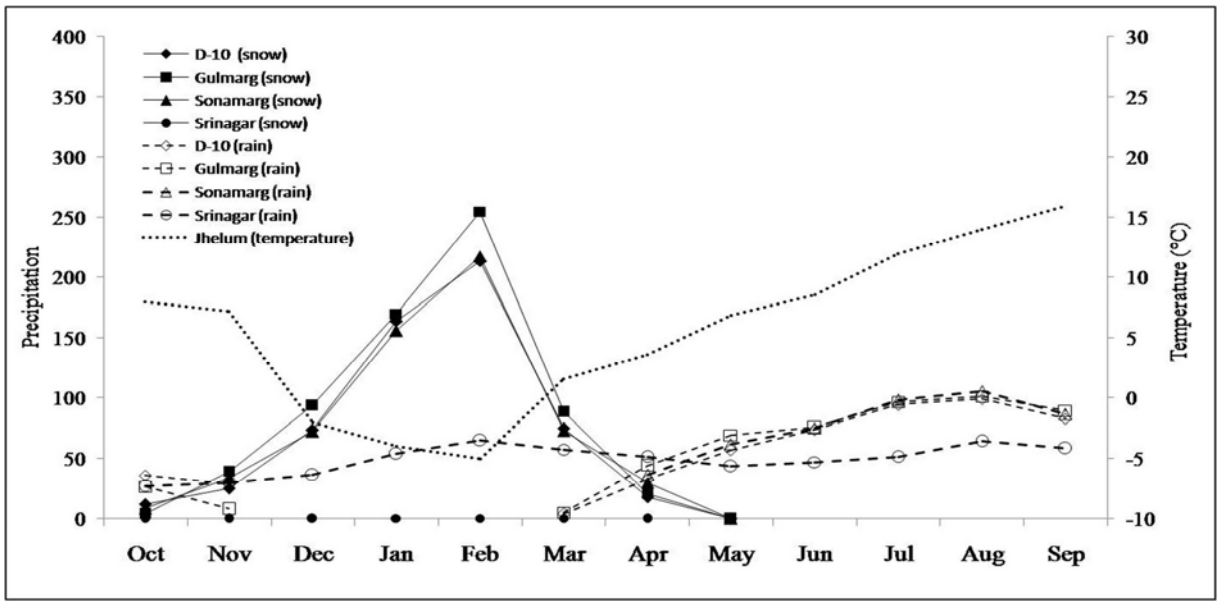

Figure 2 Average monthly temperature (°C) of Jhelum basin and average total snowfall (cm), rainfall (mm) in different observatories (Average 2000-2011)

lower latitudes covering almost entire Himalaya. This results in high snow fall precipitation in higher elevation with rainfall in lower valley region. Maximum snowfall was observed in February month (Figure 2).

The highest total seasonal snowfall was recorded in 2004-2005 (963 cm) and minimum in 2009-2010 (483 cm). Spring–summer period is characterized formation of air mass convective storms which results in intermittent rainfall in the region (Figure 2). Abundant rainfall is recorded in the entire basin during Monsoon period. The moisture laden currents of southwest monsoon travel along the Himalayas after deflected westward from the eastern Himalayan side. Reduction in the rainfall was observed with the onset of September month (Figure 2).

2 Methodology

2.1 SCE Estimation

Cloud free imageries from MODIS sensor on board Terra satellite was used for the SCE estimation. MODIS sensor scans the 2,330 km wide swath and acquires data in 36 spectral bands ranging from visible to thermal, with 12 bit radiometric resolution. All the MODIS images were geo-referenced to the Everest datum in ERDAS/ Imagine 9.1 (Leica Geosystems GIS & Mapping LLC) with sub-pixel accuracy using nearest neighborhood re-sampling technique and subsequently remaining images were georeferenced by image to image registration.

(a) Reflectance Image: Scaled integer (SI) values from satellite data were converted into the reflectance values using Equation (1) (Meng et al. 2008; Negi et al. 2008). Scaled integer values are the DN (Digital Number) values which were scaled with in a defined dynamic range so that a single set of calibration parameters can be applied for every detector in a band.

$$R_{i\lambda}\cos\theta = RS(SI - RC) \quad (1)$$

where $R_{i\lambda}$ is the spectral reflectance of a pixel; θ is the solar zenith angle in degrees; *RS* is reflectance scales; *RC* is reflectance offsets; *SI* is Scaled Integer value. Reflectance scale and reflectance offset are calibration coefficient values and can be inferred from meta information available with the satellite data (Negi et al. 2008).

(b) Snow cover maps generation: Snow cover maps of the Jhelum basin were prepared by using a well established NDSI methodology (Hall et al. 1995, 2002; Riggs and Hall 2002). NDSI has been applied and tested in the Himalayan region with good accuracy (Jain et al. 2008). In this technique, band ratioing of MODIS band -4 (green band) and band-6 (short wave infra-red) was applied on the reflectance image. Snow cover pixels were separated from non-snow pixels using Equation (2):

$$NDSI = \frac{\lambda Green \cdot \lambda SWIR}{\lambda Green + \lambda SWIR} \quad (2)$$

where $\lambda Green$ is the band-4 of MODIS (500 m pixel size); $\lambda SWIR$ is the band-6 of MODIS (500 m pixel size).

A threshold value of 0.4 (Dozier et al. 1989; Xiao et al. 2001) was used to discriminate the snow pixel using NDSI. In order to avoid merging of water bodies in the snow covered pixels criterion NDSI > 0.40 and the reflectance of MODIS band-2 (Infrared band) >11% was used (Hall et al. 2002; Jain et al. 2008).

2.2 Streamflow Simulation

(a) Streamflow simulation of entire Jhelum Basin: SRM is a widely used snow melt runoff model which can be applied on a basin of almost any size (Martinec et al. 2008). The SRM used in the study is given in Equation (3):

$$Q_{n+1} = [C_S\alpha_n(T_n + \Delta T_n)S_n + C_R P_n]A10000/86400(1 - k_{n+1}) + Q_n k_{n+1} \quad (3)$$

where Q is the average daily discharge (m^3/sec); A is the area of the basin or zone (km^2); n is the sequence of days; T_n is the number of degree days (^oC day); ΔT_n is the temperature adjustment based on lapse rate (^oC day); S_n is the ratio of SCE to total area; P is the precipitation contributing to runoff (cm); C_S is the runoff coefficient for snow; C_R is the runoff coefficient for rain; α is the degree day factor (cm/^oC/day); k is the recession coefficient indicating decline of discharge in a period without snowmelt or rainfall.

Snow cover extent was derived from satellite images using remote sensing techniques. Temperature, precipitation data recorded at various ground observatories was used. Digital

elevation model (DEM) of Advanced Spaceborne Thermal Emission and Reflection Radiometer (ASTER) with pixel size of 30 m was used to extract altitudinal zones (area elevation curve) of the basin. Snow cover depletion curves (SCDC) is a required input for accurate streamflow simulation. It represents the depleting SCE in different elevation zones during spring-summer months. SCDC can be analyzed for each elevation zone using high temporal snow cover maps, DEM and daily mean temperature. The methodology of simulating SCDC has been immensely explained by Singh et al. (2003), Martinec (2008), Jain et al. (2010), Butt and Bilal (2011). The SCDC of Jhelum river is shown in Figure 3. It shows SCDC of only 1,500 m–5,100 m altitude zones as 5,100 m–5,700 m remains permanently snow covered throughout the season.

SRM requires determined values of runoff coefficients for effective runoff simulation. The value of runoff coefficients can vary on monthly basis depending on the hydro-meteorological conditions of the basin. The runoff coefficients take care of evapotranspiration and other related runoff losses from the basin. In the present study the runoff coefficients for snow and rain were calculated (Table 3) based on the ratio of precipitation in the basin and in-situ discharge at basin outlet (Rango and Martinec 1981; Martinec and Rango 1986; Mitchell and Dewalle 1998; Martinec et al. 2008). The retrieved calculated values were adjusted until a close agreement between simulated and measured discharge was achieved.

Table 3 Runoff Coefficients (RC) of Jhelum Basin for different months

RC	Jan	Feb	Mar	Apr	May	Jun
for snow	0.14	0.11	0.30	0.58	0.61	0.66
for rain	0.12	0.33	0.20	0.32	0.37	0.38
RC	Jul	Aug	Sep	Oct	Nov	Dec
for snow	0.69	0.63	0.53	0.14	0.15	0.18
for rain	0.65	0.30	0.24	0.16	0.04	0.15

Degree day factor (α) refers to the amount of heat corresponding to 1 °C increase in temperature averaged over one day (Singh et al. 2009). It calculates the depth of daily snowmelt generated from the available number of degree-days. The

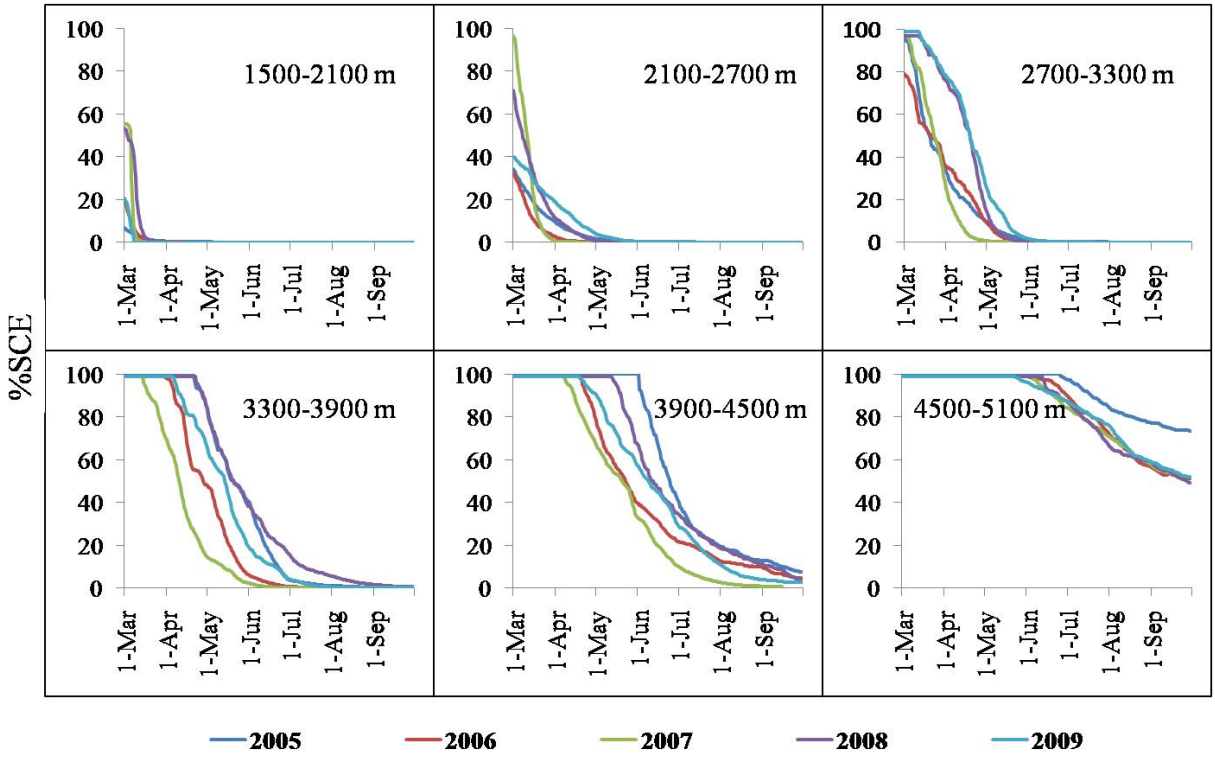

Figure 3 SCDC from 2005-2009

value of degree day was calculated using the following empirical relation (Equation (4)) (Martinec et al. 2008):

$$\alpha = 1.1\frac{\rho_S}{\rho_W} \quad (4)$$

where α is the degree day factor (cm/°C/d); ρ_s is the density of snow; ρ_w is the density of water.

The degree day factor depends on the albedo of snow. Snow crystal with high density has low albedo. Thus the snow density is an index of the changing properties which favor the snowmelt. As melt season progresses, degree day factor can go as high as 0.6 for snow and it may still be higher for glacial ice (Rango and Martinec 1979). The value of degree-day factor used in the study ranges from 0.5 to 0.6 for different months.

Recession Coefficient (k) represents decline of discharge in no rainfall and snowmelt days. It was computed for different months from historical daily discharge of Jhelum River using Equation 5 (Martinec et al. 2008):

$$k = Q_{n+1}/Q_n \quad (5)$$

where k is recession coefficient and Q_n; Q_{n+1} is the discharge value of corresponding days. The value of recession coefficient ranges between 0.9 and 1.

(b) Streamflow simulation of small ungauged sub-basin of Jhelum Basin: In the present study, the streamflow of different sub-basins and valley is simulated based on a modified snowmelt runoff model developed for small watersheds by Kulkarni et al. 2002. This model was successfully used in the Parbati, Beas and the Satluj River basins (Kulkarni et al. 2002; Singh et al. 2009). The model does not require any historical in-situ discharge observations for streamflow simulation. Thus it can be applied on the ungauged small sub-basins.

The general structure of the model used for streamflow simulation is given in Equation (6):

$$Q_{n+1} = C_{S_n}\{\alpha(T_n + \Delta T_n)S_n\} + C_{R_n}(P_n B) + C_{S_n}\{(S_n W) - (MS_W)\} \quad (6)$$

where Q is the total runoff generated (m³/s); n is the sequence of days; C_{Sn} is the runoff coefficient for snow; α is the degree day factor (cm/°C/day); T_n is the mean temperature (°C); ΔT_n is the temperature adjustment based on lapse rate (°C/day); S_n is the extent of snow (m²); C_{Rn} is the runoff coefficient for rain; P_n is the rainfall (m); W is the water equivalent of average winter snowfall (m); M is the winter snow melt (m); S_w is the Snow cover in winter (m²); B is the basin area without snow cover (m²).

The first term in Equation (6) represents quantity of seasonal snow melt during winter period (October–February) corresponding to average temperature. The second term estimates the melt due to rain. The third term in the equation is seasonal melt during summer period (March– June). The model was used assuming there is no snowfall after winter period and remaining snow cover will be melted during summer. The values of runoff coefficients and degree day factor were taken same as for the entire basin.

2.3 Accuracy assessment of simulated results

For accuracy assessment of the model, widely accepted Nash and Sutcliffe statistic test (Equation 7) was used. This test widely used to assess the predictive powers of hydrological models.

$$R^2 = 1 - \frac{\sum_i^n = 1(Q_m - Q_o)2}{\sum_i^n = 1(Q_m - Q_o'')2} \quad (7)$$

The value R^2 can range from -∞ to 1. R^2 value approaches to 1 as error reaches to zero.

The accuracy of the results was also tested with Pearson correlation test (Equation 8). It is another measure to test the strength of correlation between two variables. The Pearson coefficient is denoted by r. Its value ranges from -1 to 1.

$$r = \frac{\sum_i^n = 1(Q_m - Q_m'')(Q_o - Q_o'')}{\sqrt{\sum_i^n = 1(Q_m - Q_m'')2}\sqrt{\sum_i^n = 1(Q_o - Q_o'')2}} \quad (8)$$

where Q_m is the measured discharge; Q_o is the calculated discharge; Q_o'' is the average calculated discharge; Q_m'' is the average measured discharge; n is the no. of discharge values.

Likewise percentage difference in volume, which denotes the percentage difference between the average in-situ and simulated discharge values **(**Equation 9), was also applied for accuracy assessment of the model (World Meterological Organisation 1992; Jain et al. 2010).

$$D_{vol} = [(Q_m - Q_o)/Q_m] * 100 \quad (9)$$

where D_{vol} is the volume difference; Q_m is the measured discharge; Q_o is the calculated discharge.

The difference ranges from negative to positive values. Negative percentage difference indicates overestimation of calculated discharge whereas

positive percentage difference means underestimation of discharge values.

2.4 Stream power estimation

Stream power strongly signifies the fluvial system and meander dynamics of a river basin (Ferguson 1981; Fonstad 2003). This phenomenon is largely restrained by river geomorphic characteristics like drainage pattern, bed surface properties and sediment load. Stream power was calculated for different sub-basins of Jhelum River based on Equation 10, using slope of stream channel calculated from DEM and simulated discharge values (Bagnold 1966, 1977; Bloom 1991; Hall et al. 2012).

$$\Omega = \rho g Q S \quad (10)$$

Where ρ is the density of water (taken 1,000 kg/m^3); Q is the streamflow (m^3/sec); g is the acceleration due to gravity (9.8 m sec^{-2}); S is the channel slope.

3 Results and Discussion

3.1 Snow covers extent monitoring of Jhelum Basin

Snow cover extent is a sensitive indicator of local climatic conditions which affects regional ecological balance and anthropological activities. The Jhelum River is one of the few primarily snow-fed rivers originating in the Himalayas. Streamflow cycle of the Jhelum River is highly influenced by inter-annual and inter-seasonal snow cover variation. The present study discusses the detailed analysis of multi-temporal time series snow cover maps of the Jhelum basin and its four sub-basins: Banihal, Gulmarg, Pahalgam and Sind. Average annual SCE in the Jhelum basin estimated during 2000–2011 was 19% of the total basin area which is lower than its three sub-basins: Pahalgam (47%), Sind (45%) and Gulmarg (41%) sub basins. Inter-seasonal snow cover variation in the Jhelum basin is shown in Figure 4. Figure 4 shows that highest SCE was recorded in peak winter months suggesting the role of western disturbances in snow accumulation followed by rapid ablation during March–June months. The average SCE in past eleven years during early winter and spring-summer period remains 18% (1,780 km^2) and 22% (2,064 km^2) respectively. The maximum SCE 41% (3,926 km^2) was observed during peak winter. July onwards insignificant 2% (205) SCE observed till September end.

Figure 5 shows the inter-annual SCE variation in Jhelum basin during past decade. It shows that the maximum SCE was observed in 2004-2005 which is consistent with earlier reported observations from Western Himalaya (Negi et al. 2009; Gurung et al. 2011). A declining trend of -16% ± 3.7% was observed in Jhelum basin. The coefficient of variation (CV) calculated for seasonal SCE shows high variability for early winter period (0.31) followed by spring-summer period (0.28), monsoon period (0.21) and least in peak winter period (0.06). The low value of coefficient of variation for peak winter confirms the occurrence

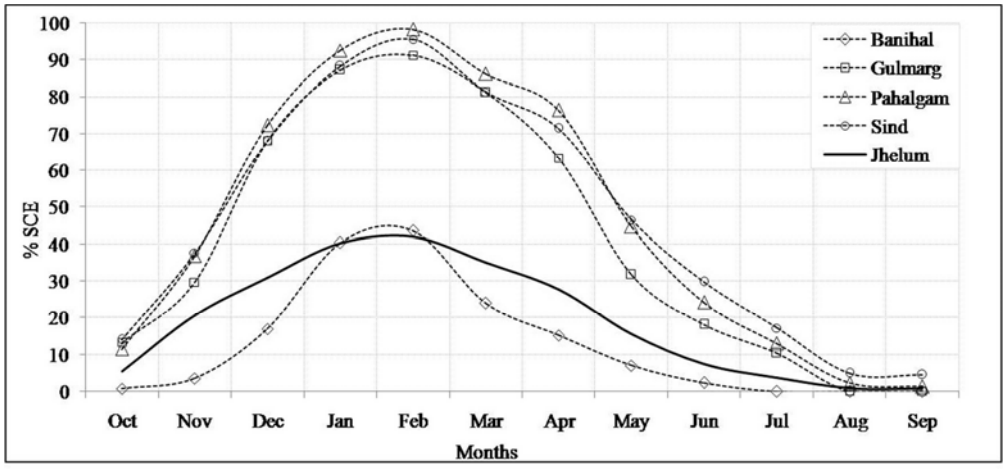

Figure 4 Average monthly SCE variation in Jhelum basin and its sub-basins in 2000-2011

of constant SCE in peak winter months. High CV values during early winter and spring-summer months can be explained by variable accumulation and ablation rate in different years.

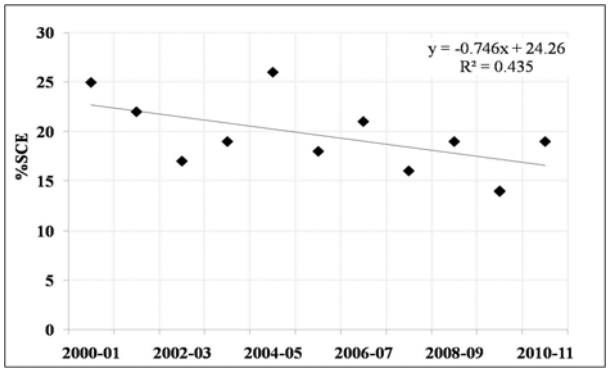

Figure 5 Decadal trend in snow cover of Jhelum basin from 2000 to 2011. The solid points illustrate mean annual SCE, and the straight line represents linear trend for the decade.

Further, extensive data analysis was carried out to understand the relationship between temperature, discharge and SCE in the basin during different seasons (Figures 6 and 7). It is evident from the results that during early winter period (October–December) close correlation (R^2 = 0.88) between the temperature and SCE exists as there was a reduction in SCE and rise in temperature (Figure 7). In this period highest temperature (3.73 °C) and least area under snow (1,331 km²) was recorded in 2007-2008, whereas, lowest temperature (1.36 °C) and maximum area under snow (2,594 km²) in the year 2004-2005 (Figure 6). In peak winter period temperature remains sub-zero causing negligible snow cover depletion. Hence low correlation (R^2 = 0.52) was observed between SCE and temperature (Figure 7).

A strong correlation (R^2 = 0.91) was observed between the SCE and the temperature in Spring–summer period (Figure 7). This period is characterized by rapid snow cover depletion. The maximum SCE (2,666 km²) was observed during spring–summer period of 2004-2005 with minimum temperature (5.84 °C). Lowest SCE (1,185 km²) was observed in 2009–2010 with highest temperatures (9.0 °C) recorded in all the years during March–June months (Figures 6 and 7). Likewise, in monsoon period (July–September) a decrease in SCE and rise in temperature were observed (R^2 = 0.87) (Figure 7). During 2004–2005 (July–September) maximum SCE (320 km²) was observed and evidently minimum temperature (13.08 °C). Likewise minimum SCE (161 km²) was observed in 2005–2006 with highest 14.68 °C temperature. The results indicate the strong implication of the air temperature on SCE variation in all the seasons except in peak winter period.

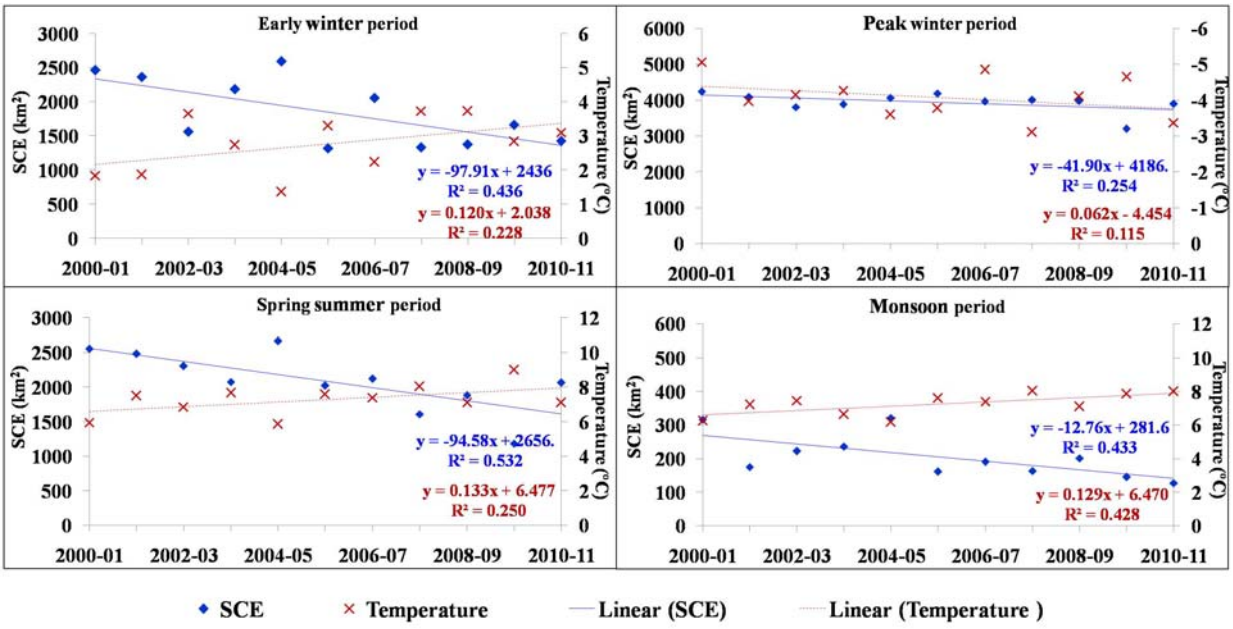

Figure 6 Mean SCE and temperature plot in various seasons in Jhelum basin during 2000-2011

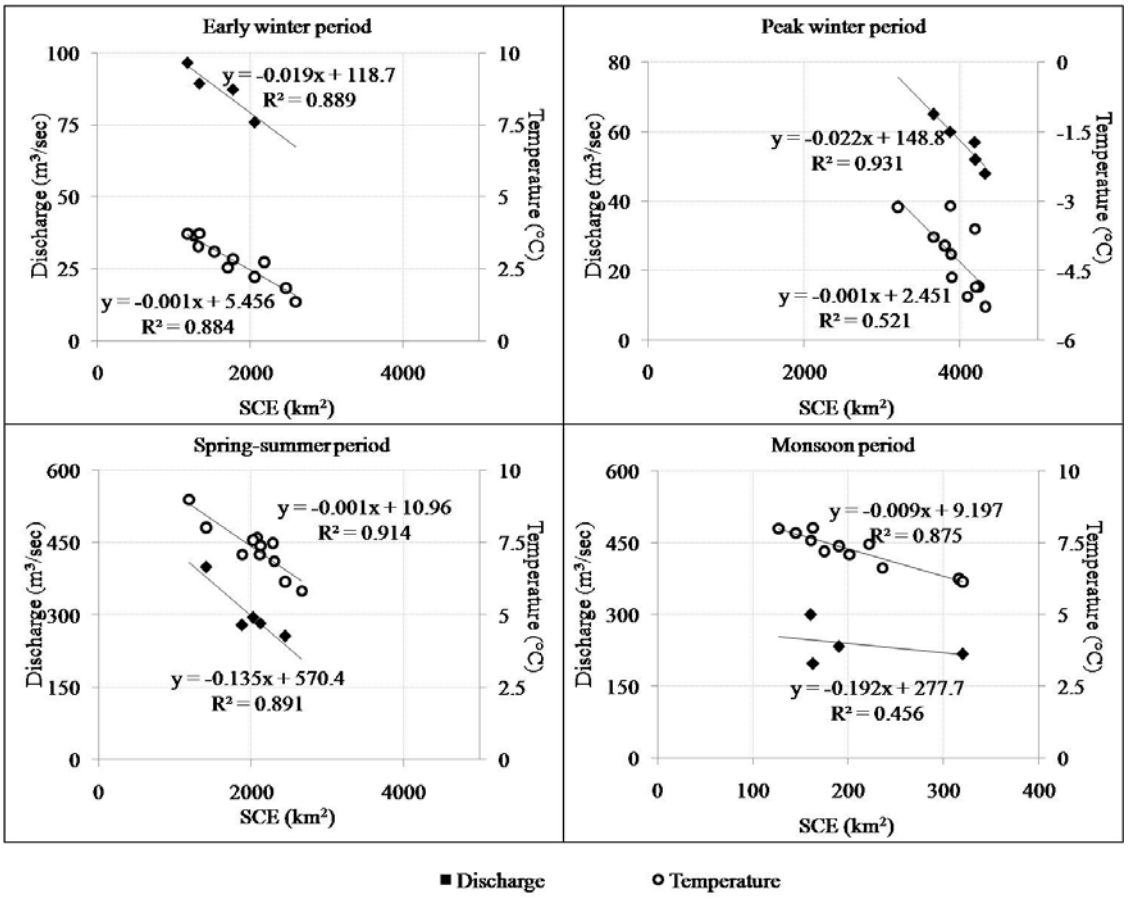

Figure 7 Correlation of average seasonal SCE with average seasonal temperature (2000-2011) and average seasonal discharge in Jhelum basin during 2005-2009.

Figure 7 shows the relationship between seasonal average SCE and discharge. During early (R^2 = 0.88) and peak winter period (R^2 = 0.93) close inverse relationship exist between the SCE and discharge. In peak winter period high snowfall, maximum SCE and low temperature are observed in the basin which results in very low discharge. During Spring-summer period discharge is significantly governed by snowmelt in the region and with decreasing SCE rapid increase in streamflow was observed (R^2 = 0.89). Monsoon period is characterized by minimal SCE, heavy rainfall, which results in high immediate peak discharge, hence low correlation (R^2 = 0.45) was observed between SCE and basin streamflow.

3.2 SCE variation in different sub-basins of the Jhelum River

Each sub basin has its own characterized SCE pattern due to the different climatic, geographic and geomorphologic conditions. Banihal lies in south-eastern end and Gulmarg in north-western tip of Pir-Panjal Range. However, Sind and Pahalgam lies in the Great Himalayan Range.

Figure 4 show SCE accumulation-ablation pattern of different sub-basins. Banihal sub-basin experiences less SCE and shortest winter span than Gulmarg, Sind and Pahalgam. Gulmarg, Pahalgam and Sind sub basins generally follows an identical snow cover distribution pattern. The snow cover accumulation period in Banihal is from November to February, whereas for other sub basins it is from October to February. Maximum snow covered extent observed in peak winter (January–February) in all sub-basins. The maximum (30%-40%) SCE observed in Banihal, (80%-90%) in Gulmarg, (80%-95%) in Pahalgam and Sind sub-basins. In March–April months, more than 50% of area remains snow covered in Gulmarg (60%-80%), Sind (70%) and Pahalgam sub-basins (75%). However, in Banihal sub basin, SCE remain less

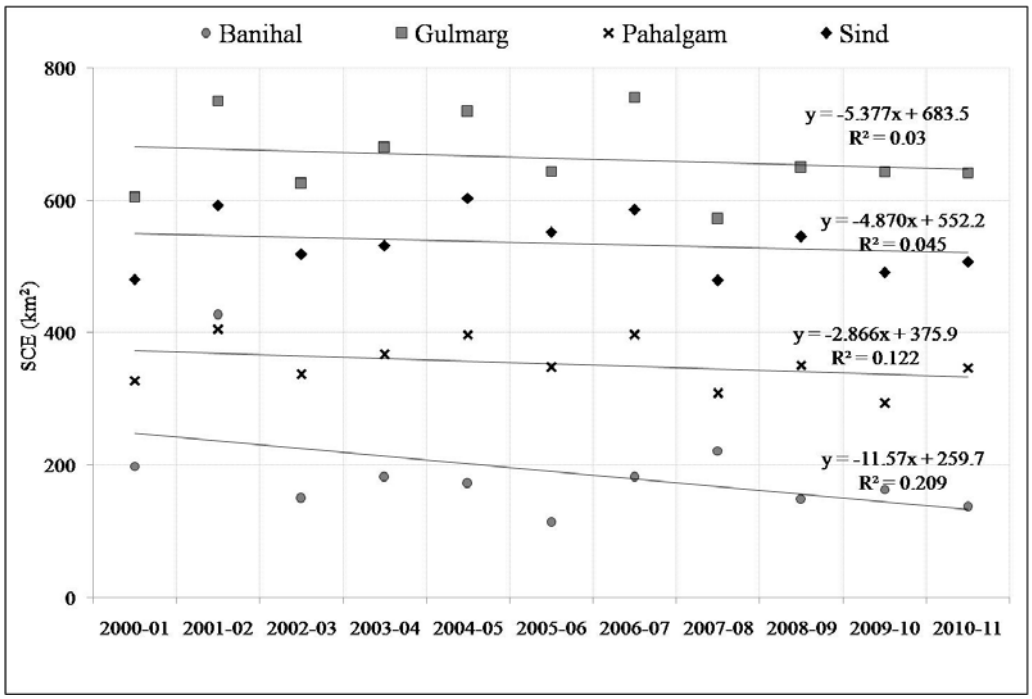

Figure 8 Decadal trend in SCE of different sub-basins form 2000 to 2011. The solid points illustrate mean annual SCE, and the straight line represents linear trend for the decade.

than 50% (15%-30%). Annual trend of mean SCE for the last eleven years (2000-2011) was analyzed for all four sub-basins and it was largely found to be declining. The maximum depletion is observed in Banihal followed by Gulmarg, Sind and Pahalgam sub-basins (Figure 8).

3.3 Stream flow estimation of Jhelum River

The comparison between daily simulated and in-situ discharge is shown in (Figure 9).

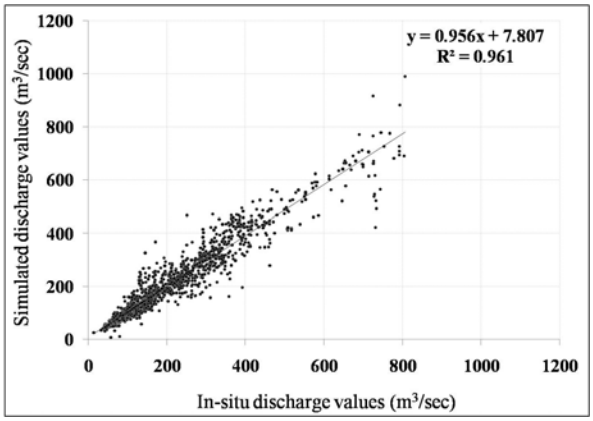

Figure 9 Nash-Sutcliffe test results for daily in-situ and simulated discharge values

High correlation coefficient value was observed between simulated and in-situ observed discharge (0.96, Nash-Sutcliffe coefficient) and (0.98, Pearson coefficient).

During early winter period (October–December) stream flow depletes from 100-55 m^3/sec due to reduction in air temperature and accumulation of snow cover. In peak winter period (January–February) estimated discharge value remains consistent and low (55 m^3/sec). Discharge during this period accounts for the contribution of baseflow from the ground water reservoirs into the river. Baseflow is the major component of the streamflow during peak winter period when no rainfall and snowmelt occurs and keeps the river perennial (Jain et al. 2010). This is the moisture amount which had infiltrated into the sub-surface zone before surface runoff generation during rain or from snow-glacial melt. Another source of baseflow is the glacial melt caused by geothermal heating from the earth surface. During spring-summer period high discharge (100 m^3/sec–750 m^3/sec) was detected. This is due to coincident snowmelt generation due to rising temperature with the intermittent rainfall. These high flow values sustains for a period of next two to three months. The seasonal snowpack is completely

Table 4 Average monthly % volume difference in in-situ and simulated discharge

Year	Jan	Feb	Mar	Apr	May	Jun	Jul	Aug	Sep	Oct	Nov	Dec
2005	-1	-2	4	5	-1	2	2	7	3	4	-3	1
2006	3	2	-5	-3	-2	-5	-6	-1	7	3	1	3
2007	1	2	-5	-5	-5	5	-5	-9	-9	0	0	-1
2008	3	2	4	-2	-3	-4	-4	7	7	0	0	1
2009	-2	-3	-5	4	3	5	3	-1	-3	--	--	--

ablated by the onset of monsoon period (July–September) but the heavy rainfall by south-west monsoons maintains the discharge value >200 m^3/sec till September end.

Table 4 shows %volume difference of the simulated and in-situ discharge in different months. It shows that during January–July the % volume difference between simulated and in-situ discharge remains < 6%. In monsoon period the maximum % difference is observed.

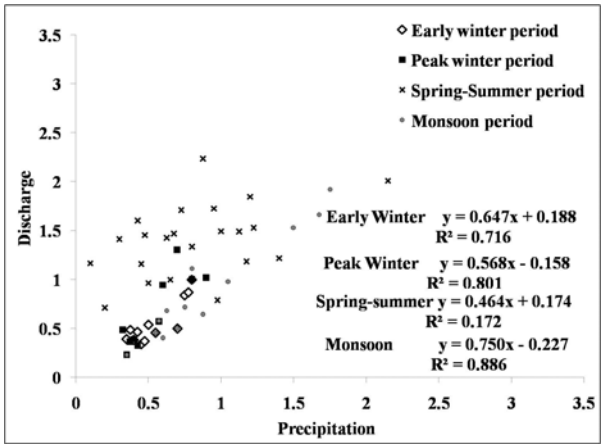

Figure 10 Relative mean precipitation and discharge correlation in various seasons in Jhelum basin during 2005-2009

The streamflow characteristics of the Jhelum River are highly influenced by the total precipitation in the basin. The hydrological relevance of precipitation with the streamflow was studied by comparing their respective relative values (Figure 10). The simulated daily discharge values were converted into relative discharge values by dividing by the annual mean discharge values. Further the resultant values are averaged at monthly scale to avoid the effect of extreme events. Figure 10 shows the correlation between relative values of discharge and precipitation in various seasons. The high coefficient of determination r^2 was observed during peak winter (0.80) and monsoon period (0.88). The correlation is very low during spring-summer period (0.17), confirming that spring streamflow is poorly explicated by spring precipitation. The result indicates that in spring-summer months the discharge of Jhelum River is majorly governed by snowmelt and in remaining months precipitation is more relevant to streamflow variation.

3.4 Streamflow simulation of different ungauged sub-basins of Jhelum River

It is evident that during different months each sub-basin contributes variable runoff to the total Jhelum river discharge. In order to evaluate runoff contribution from four ungauged sub-basins and valley region streamflow simulation for each was attempted. In this study streamflow simulation was applied for spring-summer and monsoon (March–June, July–September) as river discharge remain minimal and base flow dependent during winter season. In March month, runoff from Gulmarg basin was the major component of complete discharge due to high SCE and rising temperature leading to rapid snowmelt than other sub-basins. However, in March 2007 recorded heavy rainfall in the low-lying resulting highest discharge from valley region. During April–May variable runoff inputs from different sub-basins was observed with minimal discharge from Banihal sub-basin. Banihal sub-basin remains snow free after May and thereafter it contributes only rain induced runoff to the river discharge.

During June to September months the sub-basins with glacial cover (Sind, Pahalgam and Gulmarg) are also those with major runoff contributor during monsoon period with valley region. Banihal sub-basin is snowmelt dominated catchment and it is dependent on winter snow cover replenishment from winter precipitation. The sum of the discharge of these sub-basins has been

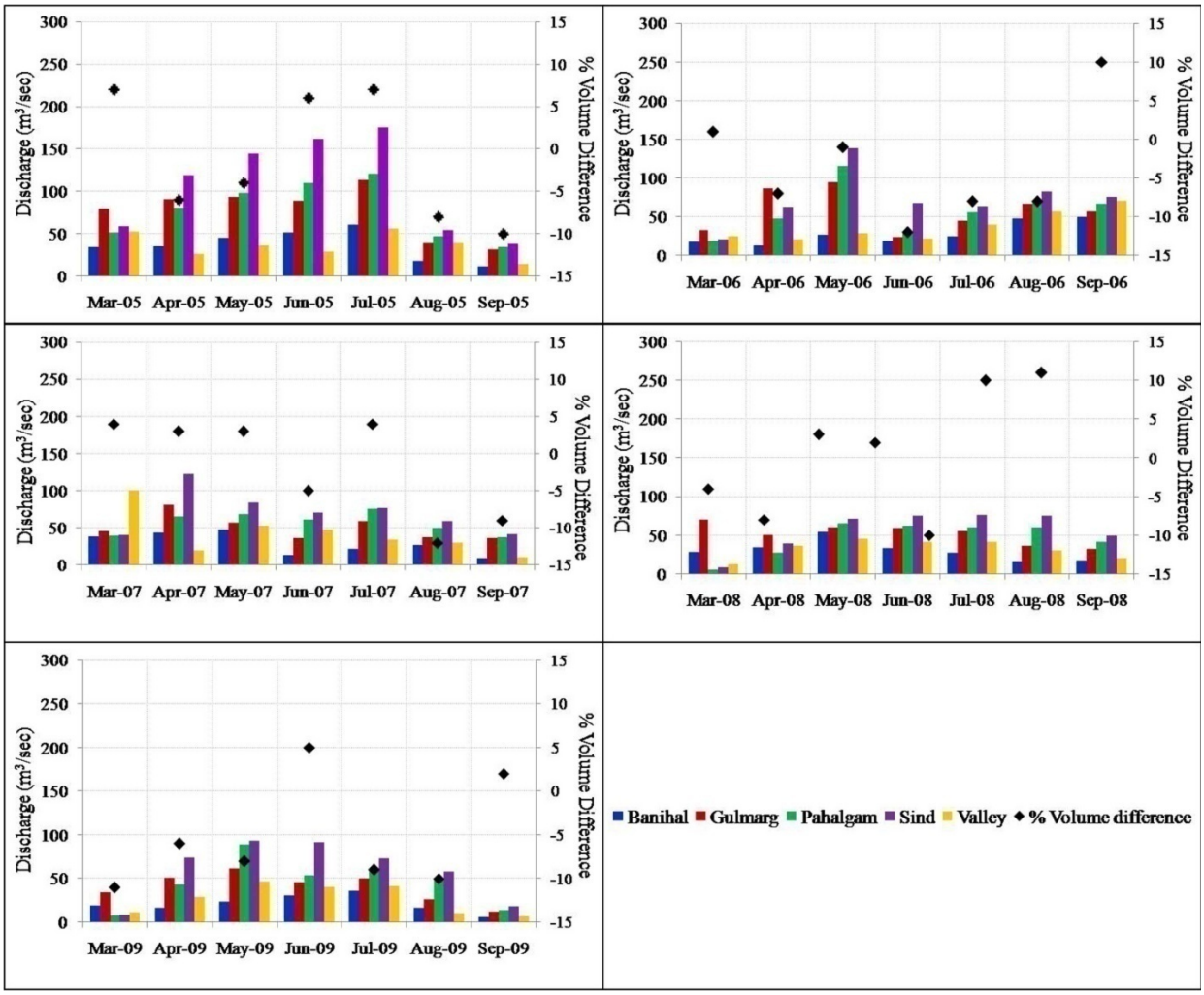

Figure 11 Monthly discharge contributions from different sub-basins and %volume difference between sum total of all sub-basin discharge and total in-situ discharge of Jhelum basin.

validated with the total discharge of the Jhelum basin (Figure 11). The results shows that the % volume difference between total discharge of Jhelum basin and summed simulated value from different sub-basins ranges from -10% to 10%.

3.5 Stream power of different sub-basins of Jhelum River

The Jhelum River is an integral part of the regional ecology. The riverscape of the Jhelum River was shaped over the time with the streams cutting steep small valleys while forming significant valley region at the bottom of the basin where the slope of the river attenuates. These streams constantly modify the bio-physical characteristics of the catchment by transporting sediments, nutrients and other crucial components from the high lands to the low-lying regions of the basin. These processes are directly linked with the catchment characteristics like stream power, basin geomorphology, drainage pattern etc. In Jhelum basin stream size increases in downstream direction and drainage pattern become more complex influencing river energy budget.

Figure 12 shows the average monthly stream power (2005-2009) for the months of March—September. The results show that Banihal sub-basin has minimum stream power because of low elevation difference and discharge within lengthy stream network. During March month highest stream power (4,600 kW/m) was observed in Gulmarg sub-basin. In this average monthly maximum discharge is also observed from Gulmarg sub-basin as discussed in earlier section. In April to September, the sub-basins with high glacial

cover and prominent stream network (Pahalgam and Sind) records maximum stream power. These two sub basins are characterized by high channel slope and steep sided valleys. During flood and heavy discharge the stream spills out of many interconnected small channels. Valley region which acts as an important catchment during monsoon period has negligible stream power due to low elevation difference and unfavorable drainage network.

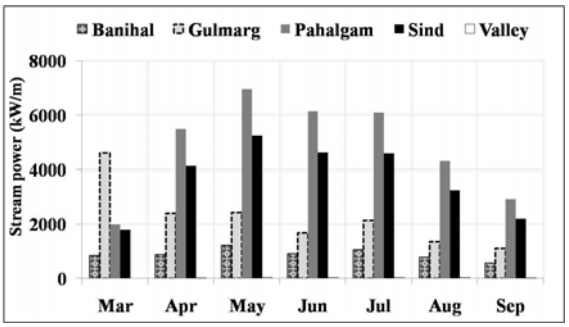

Figure 12 Average monthly stream power (2005-2009) from different sub-basins of Jhelum River

4 Conclusions

The article gives an insight about seasonal snow cover variation and different stream flow characteristics of Jhelum river basin. The study describes snow cover status and trend in the Jhelum basin in past decade. Over 40% of the total land area of the basin remains under snow in winter, which has been decreasing over past decade as indicated by declining trend between years 2000 and 2011. Inter-annual and inter-seasonal SCE trends have also shown a decreasing trend. Further in agreement with the earlier reported studies from Western Himalaya SCE during spring-summer is also decreasing. The study reveals that each sub-basin has different basin conditions which significantly governs accumulation and ablation pattern of SCE. This finding supports the fact that snow cover in north-west Himalayas varies at different spatial scales considerably and basin characteristics plays an important role in snow cover changes. An inverse strong correlation between satellite derived SCE and in-situ temperature data shows consistency with similar studies conducted in Bhutan and China (Pu et al. 2007; Gurung et al. 2011). This further establishes the influence of temperature on snow cover variation and suggests that the decline in SCE is due to increase in mean temperature. The SCE-streamflow shows strong correlation in different seasons except in monsoon period highlighting the influence of rainfall on monsoonal discharge. Hydrological relevance of the basin precipitation with the streamflow was studied by comparing their respective relative values. It suggests that seasonal SCE is a prime factor governing streamflow during spring-summer period.

The potential of SRM model for the streamflow simulation in Jhelum Basin was assessed and a good correlation between estimated and in-situ discharge was found. Further, SRM model can be used to evaluate the effects of climate change on the Jhelum basin by integrating futuristic climate change scenarios. It was revealed that the baseflow contribution during peak winter period remains ~ 55 (m^3/sec) in the total discharge of Jhelum. Further in the study the streamflow of all four ungauged sub-basins and valley region was simulated using a runoff model developed for the small ungauged watersheds. It was observed that sum of simulated discharge from different sub-basins was comparable to the total discharge of the Jhelum basin. The study suggest that applied model is an important tool for studies related to water allocation, irrigation, hydropower potential estimation and climate change for snow-fed ungauged basins. Stream power of different sub-basins was also estimated. Stream power is of paramount importance in determination of stream characteristics like sediment load, nutrient carrying capacity etc. of a river basin. The results provides glance of geographical variation of stream power in Jhelum basin. Important spatial variability in the stream power of different sub basins within the study area was observed. This difference is in accordance with elevation difference, average streamflow and stream network of different catchment.

Acknowledgements

The authors are grateful to Sh. Ashwagosha Ganju, Director, Snow and Avalanche Study Establishment (SASE) for providing facilities to carry out this work and constant motivation during

the investigation. The authors also like to express their sincere thanks to all scientists and scientific assistants who were involved in collection field data and Central Water Commission (CWC) for providing the Jhelum River discharge data. Special thanks to Sh. Narinder Kumar Thakur, Technical Officer, SASE for fruitful discussions about the study.

References

Archer DR, Fowler HJ (2004) Spatial and temporal variations in precipitation in the Upper Indus Basin, global teleconnections and hydrological implications. Hydrology and Earth System Sciences 8: 47–61.

Archer DR, Fowler HJ (2008) Using meteorological data to forecast seasonal runoff on the River Jhelum, Pakistan. Journal of Hydrology 361: 10–23.

Bagnold RA (1966) An approach to the sediment transport problem from general physics. Geological Survey Professional Paper 422(1): 11–137.

Bangnold RA (1977) Bedload transport by natural rivers. Water Resources Research 13: 303–312.

Blandford HF (1884) On the connexion of the Himalaya snowfall with dry winds and seasons of drought in India. Proceedings of the Royal Society of London 37: 1–23.

Bloom A (1991) Geomorphology: a systematic analysis of late Cenozoic landforms. Prentice Hall, Englewood Cliffs, New Jersey. pp 236–237.

Butt M, Bilal M (2011) Application of snowmelt runoff model for water resource management. Hydrological Processes 25(24): 3735-3747. DOI: 10.1002/hyp.8099.

Dozier J (1989) Spectral signature of alpine snow cover from the Landsat Thematic Mapper. Remote Sensing of Environment 28: 9–22.

Ferguson RI (1981) Channel forms and channel changes. In: Lewin J (Ed.). British Rivers. G Allen & Unwin, London. pp 90–125.

Fitzharris BB, Mcalevey BP (1999) Remote sensing of seasonal snow cover in the mountains of New Zealand using satellite imagery. Geocarto International 14: 35–40.

Fonstad MA (2003) Spatial variation in the power of mountain streams in the Sangre de Cristo Mountains, New Mexico. Geomorphology 55: 75–96.

Foster J, Liston G, Koster R, et al. (1996) Snow cover and snow mass intercomparison of general circulation models and remotely sensed data sets. Journal of Climate 9: 409–426.

Gurung DR, Kulkarni AV, Giriraj A, et al. (2011) Monitoring of seasonal snow cover in Bhutan using remote sensing technique. Current Science 101(10): 1364-1370.

Hall DK, Riggs GA, Salomonson VV (1995) Development of methods for mapping global snow cover using Moderate Resolution Imaging Spectroradiometer (MODIS) data. Remote Sensing of Environment 54(2): 127–140.

Hall DK, Riggs GA, Salomonson VV, et al. (2002) MODIS snow cover products. Remote Sensing of Environment 83: 181–194.

Hall DK, Foster JL, DiGirolamo NE, Riggs GA (2012) Snow cover, anowmelt timing and stream power in the Wind River Range, Wyoming. Geomorphology 137: 87–93.

Homan JW, Luce CH, Mcnamara JP, et al. (2011) Improvement of distributed snowmelt energy balance modeling with MODIS-based NDSI-derived fractional snow-covered area data. Hydrological Processes 25: 650–660.

Immerzeel WW, Droogers P, Jong DE SM, et al. (2009) Large Scale monitoring of snow cover and run-off simulation in Himalayas river basins using remote sensing. Remote sensing of Environment 113: 40–49.

Jain SK, Kumar N, Ahmad T (1998) SLURP model and GIS estimation of runoff in a part of Satluj catchment, India. Hydrological Sciences 43: 875–884.

Jain SK, Goswami A, Saraf AK (2008) Accuracy assessment of MODIS, NOAA, and IRS data in snow cover mapping under Himalayan conditions. International Journal of Remote Sensing 29: 5863–5878.

Jain SK, Goswami A, Saraf AK (2009) Role of elevation and aspect in snow distribution in Western Himalaya. Water resource Management 23: 71–83.

Jain SK, Goswami A, Saraf A (2010) Snowmelt runoff modelling in a Himalayan basin with the aid of satellite data. International Journal of Remote Sensing 31: 6603–6618.

Kriplani RH, Kulkarni S, Sabade S (2004) Western Himalayan snowcover and Indian monsoon rainfall: A re-examination with INSAT and NCEP/NCAR data. Theoritical and Applied Climatology 74: 1–18.

Kulkarni AV, Randhawa SS, Rathore BP, et al. (2002) Snow and Glacier Melt Runoff Model to Estimate Hydropower Potential. Journal of Indian Society of Remote Sensing 30: 221–228.

Kulkarni AV, Singh SK, Mathur P, et al. (2006) Algorithm to monitor snow cover using AWiFS data RESOURCESAT-1 for the Himalayan region. International Journal of Remote Sensing 27: 2449–2457.

Kumar SK, Haefner H, Seidel K (1991) Satellite snow cover mapping and snowmelt runoff modeling in Beas basin. Proceedings of the Vienna Symposium*, August 1991*, IAHS Publ. no. 205: pp 101–109.

Li XG, Williams MW (2008) Snowmelt runoff modeling in an arid mountain watershed, Tarim Basin, China. Hydrological Processes 22(19): 3931-3940. DOI: 10.1002/hyp.7098

Mitchell KM, Dewalle DR (1998) Application of the snowmelt runoff model using multiple parameter landscape zones on the Towanda creek basin, Pennsylvania. Journal of the American Water Resources Association 34: 335–346.

Martinec J (1975) Snowmelt Runoff Model for streamflow forecasts. Nordic Hydrology 6(3): 145–154.

Martinec J, Rango A (1986) Parameter values for snowmelt runoff modeling. Journal of Hydrology 84: 197–219.

Martinec J, Rango A, Roberts R (2008) Snowmelt Runoff Model (SRM) User's Manual (version 1.11) Available online: http://hydrolab.arsusda.gov/cgi-bin/srmhome/srm4.pdf (accessed on 10 November 2011)

Maurer EP, Rhoads JD, Dubayah RO, et al. (2003) Evaluation of the snow covered area data product from MODIS. Hydrological Processes 17: 59–71

Meng L, Tao L, Li J, et al. (2008) A system for automatic processing of MODIS L1B data. 8th International Symposium on spatial accuracy assessment in Natural Resources and Environmental Sciences, June 2008, Shanghai, China. pp 335–343.

Negi HS, Snehmani, Thakur NK (2008) Operational Snow Cover Monitoring in NW-Himalaya using Terra and Aqua MODIS Imageries. Proceedings International Workshop on Snow, Ice, Glacier and Avalanches, IITMumbai, India, 7–9 January 2008. pp 11–25.

Negi H, Thakur N, Kumar R, et al. (2009) Monitoring and evaluation of seasonal snow cover in Kashmir valley using remote sensing, GIS and ancillary data. Journal of Earth System and Science 118(6): 711–720.

Prasad VH, Roy PS (2005) Estimation of Snowmelt Runoff in Beas Basin, India. Geocarto International 20: 41–47.

Pu Z, Xu L, Salomonson V (2007) MODIS/Terra observed seasonal variations of snow cover over the Tibetan Plateau.

Geophysical Research Letters 34: 1-6.
Ramamoorthi AS, Haefner H (1991) Runoff Modeling and Forecasting of River Basins, and Himalayan Snowcover Infromation (HIMSIS). Proceedings of the Vienne Symposium, IAHS Publ. no 201. pp 347–355.
Rango A, Martinec J (1979) Application of a snowmelt-runoff model using satellite data. Nordic Hydrology 10: 225–238.
Rango A, Martinec J (1981) Accuracy of snow melt runoff simulation. Nordic Hydrology 12: 265–274.
Rathore, BP, Kulkarni AV, Sherasia NK (2009) Understanding future changes in snow and glacier melt runoff due to global warming in Wangar Gad basin, India. Current Science 97: 1077–1081.
Riggs H, Hall DK (2002) Reduction of cloud obscuration in the MODIS snow data product. 59th Eastern Snow conference, 5–7 June 2002, Stowe, Vermont USA. pp 205–212.
Rutger D, Steven M, De J (2004) Monitoring snow-cover dynamics in northern Fennoscandia with SPOT VEGETATION images. International Journal of Remote Sensing 25: 2933–2949.
Salomonson VV, Appel I (2004) Estimating fractional snow cover from MODIS using the normalized difference snow index. Remote Sensing of Environment 89: 351–360.
Shaman J, Tziperman E (2005) The effects of ENSO on Tibetan plateau snow depth: A stationary wave teleconnection mechanism and implication for the South Asian monsoons. Journal of Climate 18: 2067–2079.
Singh P, Quick MC (1993) Streamflow simulation of Satluj River in the Western Himalayas. Snow and Glacier Hydrology, IAHS publication no.218. pp 261–271.
Singh M, Mishra VD, Thakur NK, et al. (2009) Impact of climatic parameters on statistical steam flow sensitivity analysis for Hydropower. Journal of Indian Society of Remote Sensing 37: 573–586.
Tekeli AE, Akyurek Z, Sorman AA, et al. (2005) Using MODIS snow cover maps in modelling snowmelt runoff process in the eastern part of Turkey. Remote Sensing of Environment 97: 216–230.
Trujilo E, Ramirez JA, Elder KJ (2007) Topographic meteorological, and canopy controls on the scaling characteristics of the spatial distribution of snow depth fields. Water Resources Research 43: 1–17.
Verdhen A, Prasad T (1993) Snowmelt Runoff Simulation Models and their Suitability in Himalayan Conditions, Snow and Glacier Hydrology (Proceedings of the Kathmandu Symposium), IAHS Publ. no. 218. pp 239–248.
Xiao XM, Shen ZX, Qin XG (2001) Assessing the potential of VEGETATION sensor data for mapping snow and ice cover: A normalized mapping snow and ice index. International Journal of Remote Sensing 22: 2479–2487.
Xiao X, Moore B, Qin X, et al. (2002) Large-scale observation of alpine snow and ice cover in Asia, using multi-temporal VEGETATION sensor data. International Journal of Remote Sensing 23(11): 2213–2228.
Xiao X, Zhang Q, Boles S, et al. (2004) Mapping snow cover in the Pan-Arctic zone using multi-year (1998–2001) images from optical VEGETATION sensor. International Journal of Remote Sensing 25(24): 5731–5744.
Yang ZL, Dickinson RE, Hahmann AN, et al. (1999) Simulation of snow mass and extent in general circulation models. Hydrological Processes 13: 2097–2113.
Zhang HE, Zhao JF, Shi JC (2005) Comparing four sub-pixel Algorithms in MODIS Snow mapping. International Geoscience and Remote Sensing Symposium 6: 3784–3787.
Zhang YZ, Yan S, Lu Y (2010) Snow cover Monitoring Using MODIS Data in Liaoning Province, Northeastern China. Remote Sensing 2(3): 777-793.
World Meterological Organization (1992) Simulated real-time intercomparison of hydrological models. Operational Hydrology Report 38 WMO No. 779, Geneva Switzerland.